THE FASEB JOURNAL • RESEARCH • www.fasebj.org

Targeting the Stat6 pathway in tumor-associated macrophages reduces tumor growth and metastatic niche formation in breast cancer

Karin Binnemars-Postma,* Ruchi Bansal,* Gert Storm,*,† and Jai Prakash*,[1]

*Targeted Therapeutics, Biomaterials Science and Technology, Institute for Biomedical Technology and Technical Medicine (MIRA), University of Twente, Enschede, The Netherlands; and †Department of Pharmaceutics, Utrecht University, Utrecht, The Netherlands

ABSTRACT: Tumor-associated macrophages (TAMs) are the key effector cells in the tumor microenvironment and induce neoangiogenesis, matrix remodeling, and metastasis while suppressing the tumor immune system. These protumoral macrophages display an M2 phenotype induced by IL-4 and IL-13 cytokines. In this study, we hypothesized that the inhibition of the signal transducer and activator of transcription 6 (Stat6) pathway, a common downstream signaling pathway of IL-4 and IL-13, may be an interesting strategy by which to inhibit TAM differentiation and, thus, their protumorigenic activities. *In vitro* inhibition of the Stat6 pathway by using small interfering RNA or the pharmacologic inhibitor, AS1517499, inhibited the differentiation of mouse RAW264.7 macrophages into the M2 phenotype, as demonstrated by the reduction of *Arg-1* (arginase-1) and *Mrc-1* (mannose receptor 1) expression and arginase activity. *In vivo*, AS1517499 significantly attenuated tumor growth and early liver metastasis in an orthotopic 4T1 mammary carcinoma mouse model. Furthermore, in another experiment, we observed an increase in the intrahepatic mRNA expression of *F4/80* (EGF-like module-containing mucin-like hormone receptor-like 1; total macrophages) and M2 macrophage markers [*Ym-1* (chitinase 3–like protein 3) and *Mrc-1*] and metastatic niche markers [*Mmp-2* (matrix metalloproteinase-2), *Postn* (periostin), and *Cd34*] in mice with increasing growth of primary tumors. Of interest, these markers were found to be reduced after treatment with AS1517499. In summary, inhibition of the Stat6 pathway in TAMs is a vital therapeutic approach to attenuate tumor growth and metastasis by inhibiting TAM-induced protumorigenic and prometastatic activities.—Binnemars-Postma, K., Bansal, R., Storm, G., Prakash, J. Targeting the Stat6 pathway in tumor-associated macrophages reduces tumor growth and metastatic niche formation in breast cancer. FASEB J. 32, 969–978 (2018). www.fasebj.org

KEY WORDS: TAMs · AS1517499 · M2 macrophages · liver metastasis

Breast cancer, with almost 1.7 million new diagnoses and more than half a million deaths in 2012, is the most common type of cancer in women worldwide (1). Increasing evidence has demonstrated a relationship between a high degree of macrophage infiltration and poor prognosis in human breast cancer and other malignancies, which suggests that macrophages play an important role in tumor progression and metastasis in cancer (2–5). Macrophages are myeloid cells that show a high degree of plasticity, commonly defined as two distinct phenotypes—classically activated M1 macrophages, which have proinflammatory and antitumoral effects, and alternatively activated M2 macrophages, which display immunosuppressive, wound-healing, and protumoral characteristics (6–8). Macrophage polarization state is determined by external stimuli that are present within the tissue microenvironment (9). Tumor-associated macrophages (TAMs), displaying the M2 phenotype, play a critical role in tumor survival, growth, and metastasis (10, 11). TAMs originate from either resident macrophages or infiltrated monocytes from the circulation to the tumor site. Tumor cells secrete such cytokines as IL-4, IL-13, and IL-10, which are able to polarize infiltrated macrophages into TAMs (7).

Upon acquisition of the TAM phenotype, these macrophages support tumor growth and progression by performing numerous protumoral activities: stimulation of neoangiogenesis, matrix remodeling, excretion of growth factors, and suppression of the immune system (7, 10, 12, 13). TAMs have therefore become a key target cell type for the development of antitumor therapies. Studies have demonstrated that the depletion

ABBREVIATIONS: *Arg-1*, arginase-1; F4/80, EGF-like module-containing mucin-like hormone receptor-like 1; Mmp-2, matrix metalloproteinase 2; Mrc-1, mannose receptor 1; Postn, periostin; siRNA, small interfering RNA; Stat6, signal transducer and activator of transcription 6; TAM, tumor-associated macrophage; Ym-1, chitinase 3–like protein 3

[1] Correspondence: University of Twente, Drienerlolaan 5, 7522 NB Enschede, The Netherlands. E-mail: j.prakash@utwente.nl

doi: 10.1096/fj.201700629R

This article includes supplemental data. Please visit *http://www.fasebj.org* to obtain this information.

of TAMs by using bisphosphonate-loaded liposomes leads to the inhibition of tumor growth and metastasis (14, 15); however, the nonselective depletion of macrophages may lead to worse overall outcomes, as macrophages also display antitumor activities (16). Other strategies aimed at the treatment of TAMs include the targeting of the colony-stimulating factor-1 receptor, which plays a critical role in the migration, differentiation, and survival of macrophages (17). A recently investigated compound, BLZ-945, a colony-stimulating factor-1 receptor inhibitor, was shown to inhibit TAM differentiation and tumor growth in a murine model for glioblastoma (18); however, Quail *et al.* (19) recently demonstrated that treatment with BLZ-945 resulted in resistance and 56% of mice displayed tumor recurrence as a result of tumor microenvironment–derived factors. On the one hand, these findings advance our knowledge of TAM-based therapies, but, on the other hand, trigger the need to develop new therapies in this direction.

The signal transducer and activator of transcription 6 (Stat6) pathway is a common signaling pathway for cytokines IL-4 and IL-13—the key cytokines for TAM polarization. These cytokines, secreted within the tumor microenvironment, bind to their receptors, IL-4Rα and IL-13Rα1, respectively, and activate the Jak/Stat pathway (phosphorylation of Stat6), which results in the translocation of pStat6 to the nuclei (6, 20). Once located in the nucleus, Stat6 activates the transcription of target genes that are specific for M2 macrophages, such as mannose receptor 1 (*Mrc-1*), resistin-like α (*Retnla*, *Fizz1*), chitinase 3-like 3 (*Chi3l3*), and chitinase 3–like protein 3 (*Ym-1*) (9, 21); therefore, Stat6 inhibition in TAMs might inhibit their protumorigenic phenotype. In addition, there is evidence that the deletion of the Stat6 gene facilitates the development of potent antitumor immunity *via* a $CD4^+$-independent pathway in a 4T1 mouse tumor model (22). Furthermore, Krüppel-like factor 4, a member of the subfamily of the zinc-finger class of DNA-binding transcriptional regulators, upon activation by Stat6, inhibits the hypoxia-inducible factor-1α /NF-κB pathway, which plays an important role in the activation of M1 macrophages (23). Activation of Stat6 thus has a dual effect on macrophage differentiation *via* the induction of M2-associated gene transcription and the inhibition of M1-associated signaling pathways.

As Stat6 plays an important role in the differentiation of TAMs and in the regulation of tumor immunity, we hypothesized that Stat6 may represent an interesting therapeutic target by which to inhibit TAM-induced protumorigenic activities. In the present study, we first examined the activation of the Stat6 pathway in human patient breast tumor tissue and a mouse tumor model. We then investigated the effect of silencing Stat6 in murine M2 macrophages *in vitro*. To investigate the effect of the pharmacologic inhibition of the Stat6 pathway, we used the inhibitor AS1517499—previously used in models for antigen-induced bronchial hyper-reactivity (24–26)—and studied its effects on TAM differentiation *in vitro* and on tumor growth and metastasis in a 4T1 mammary carcinoma mouse model *in vivo*.

MATERIALS AND METHODS

Cell lines

Mouse RAW264.7 macrophages were obtained from the American Type Culture Collection (Manassas, VA, USA). 4T1-luc breast cancer cells were kindly provided by Dr. O. van Tellingen (Netherlands Cancer Institute, Amsterdam, The Netherlands). Both cell lines were cultured in RPMI 1640 medium that was supplemented with 10% fetal bovine serum, 2 mM L-glutamine (Lonza, Basel, Switzerland), and 100 U/ml penicillin and 0.1 mg/ml streptomycin (Sigma-Aldrich, St. Louis, MO, USA). Anonymous human breast tumor tissue was provided by Dr. van Baarlen (LabPON, Hengelo, The Netherlands).

Macrophage differentiation

M1 macrophages were differentiated by using murine recombinant IFN-γ and LPS (055:B5; Sigma-Aldrich), both at 10 ng/ml. M2 macrophages were differentiated by using 10 ng/ml murine recombinant IL-4 and IL-13. All cytokines were obtained from PeproTech (London, United Kingdom). M1 differentiation of macrophages was determined by measuring the accumulation of NO_2 nitrite in the medium of differentiated cells. Cells were seeded in 96-well plates. After starvation, cells were incubated with differentiation medium. After 24 h, NO_2 concentration was measured at 540 nm by using a Griess reagent [200 mg sulfanilamide (Sigma Aldrich), 20 mg *N*-naphthylethylenediamine dihydrochloride (Sigma Aldrich) and 0.5 ml of phosphoric acid (Thermo Fisher Scientific, Waltham, MA, USA) per 20 ml solution in water]. M2 differentiation of macrophages was determined by measuring arginase-1 activity in the cell lysates of differentiated cells. In brief, cell lysate was activated by 10-min incubation at 55°C using 10 mM $MnCl_2$/50 mM Tris-HCl (pH 7.5) solution. Activated lysate was mixed with 0.5 M L-arginine (pH 9.7) solution and incubated for 24 h at 37°C. The reaction was stopped with the addition of 8.7% H_2SO_4 and 23.2% H_3PO_4 in water solution. Color was developed by incubating at 100°C for 1 h using 9% α-isonitrosopropiophenone in ethanol solution and measuring absorbance at 545 nm.

Real-time quantitative PCR

Cells were differentiated using the method previously described. The Stat6 inhibitor, AS1517499 [4-(benzylamino)-2-(3-chloro-4-hydroxyphenethylamino)pyrimidine-5-carboxamide; Axon Medchem, Groningen, The Netherlands], was added in concentrations of 10, 100, and 250 nM, and cells were incubated for 24 h. Total RNA was isolated by using the GenElute Mammalian Total RNA Miniprep Kit (Sigma-Aldrich). RNA was isolated from mouse tumors and livers by using the SV Total RNA Isolation System (Promega, Madison, WI, USA). cDNA was prepared by using an iScript cDNA synthesis kit (Bio-Rad, Hercules, CA, USA). Primer sequences are listed in **Table 1**. Reactions were measured by using the CFX384 Real-Time PCR Detection System (Bio-Rad). Threshold cycles (C_t) were calculated and relative gene expression was analyzed after normalization with the glyceraldehyde 3-phosphate dehydrogenase (*Gapdh*) housekeeping gene.

Cell viability

RAW264.7 cells were grown under experimental conditions as previously described. 4T1-luc cells were seeded at a cell density of 5×10^4 cells/ml. After 24 h of culturing, cells were starved overnight and subsequently treated with increasing concentrations

TABLE 1. *Sequences of primers used for gene expression using real-time quantitative PCR*

Gene	Primer, 5′–3′ Forward	Reverse	Accession
Arg-1	GTGAAGAACCCACGGTCTGT	CTGGTTGTCAGGGGAGTGTT	NM_007482.3
Cd34	GGGTAGCTCTCTGCCTGATG	TCTCTGAGATGGCTGGTGTG	NM_133654.3
Cd4	TTCCCTCCCTCTGTTCCCAA	GCCCTCTCGTAAACTGTGCT	NM_013488.2
Cd8	CACAAATGATCAGCGCCCAC	CAGCAGTTCAAAGCAGGCAG	NM_009858.2
F4/80	TGCATCTAGCAATGGACAGC	GCCTTCTGGATCCATTTGAA	NM_010130.4
FoxP3	CCCAGGAAAGACAGCAACCTT	TTCTCACAACCAGGCCACTTG	NM_001199348.1
Gapdh	ACAGTCCATGCCATCACTGC	GATCCACGACGGACACATTG	XM_001476707.3, XM_001479371.4, XM_003946114.1, NM_008084.2
Il-1β	GCCAAGACAGGTCGCTCAGGG	CCCCCACACGTTGACAGCTAGG	NM_008361.3
Il-6	TGATGCTGGTGACAACCACGGC	TAAGCCTCCGACTTGTGAAGTGGTA	NM_031168.1
Mrc-1	GGGACGTTTCGGTGGACTGTGG	TTGTGGGCTCTGGTGGGCGA	NM_008625.2
Mmp-2	TTTCTATGGCTGCCCCAAGG	GTCAAGGTCACCTGTCTGGG	NM_008610.2
Postn	ATCCACGGAGAGCCAGTCAT	TGTTTCTCCACCTCCTGTGG	NM_001198766.1
Stat6	GTTTACAGTGAAGAAGGCCCG	CTGGGCTGGCCCTAAAAACT	NM_009284.2
Ym-1	ACTTTGATGGCCTCAACCTG	AATGATTCCTGCTCCTGTGG	NM_009892.2

of AS1517499. After treatment with AS1517499 at different concentrations for 24 h, the medium was aspirated and replaced with a 10% resazurin sodium salt (Sigma-Aldrich) solution (110 μg/ml) in culture medium without fetal bovine serum. Cells were cultured for an additional 1–4 h. Medium was collected and measured by using the Victor3 Multilabel Plate Reader (PerkinElmer, Waltham, MA, USA).

Gene silencing

Twenty-four hours after seeding, RAW264.7 cells were transfected by using Stat6 small interfering RNA (siRNA) or scrambled control siRNA (Santa Cruz Biotechnology, Dallas, TX, USA) at a concentration of 10 nM, combined with HiPerFect (Qiagen, Venlo, The Netherlands) transfection reagent per manufacturer instructions. After 24 h of transfection, cells were differentiated and harvested for gene expression and arginase activity as previously described.

Western blotting

To determine the effect of AS15171499 on the inhibition of Stat6 phosphorylation, cells were differentiated and treated with AS1517499, whereas 4T1-luc cells remained untreated. Western blot analysis was performed according to a standard protocol. In brief, cells were lysed by using lysis buffer, and equal amounts of samples were loaded onto 10% Tris-glycine gels (Thermo Fisher Scientific) and transferred to PVDF membranes (Thermo Fisher Scientific). Blots were probed with anti-Stat6 or anti-pStat6 Abs (Cell Signaling Technology, Danvers, MA, USA) by overnight incubation at 4°C, followed by incubation at room temperature for 1 h with species-specific horseradish peroxidase–conjugated secondary Ab. Proteins were detected by using a Pierce ECL Plus Western Blotting Substrate kit (Thermo Fisher Scientific) and were exposed to the FluorChem M System (Protein Simple, Kanata ON, Canada). Target protein levels were quantified by using ImageJ software (National Institutes of Health, Bethesda, MD, USA).

In vitro paracrine effects of treated differentiated macrophages on 4T1-luc breast cancer cells

Cells were differentiated and treated with AS1517499. After 24 h of differentiation, the medium was removed and cells were washed thoroughly. New medium without cytokines was added, and conditioned medium was collected after 24 h of incubation. For the wound-healing assay, 4T1-luc cells were seeded in 24-well plates. Cells were starved overnight and a scratch was made in the middle of the well. Cells were washed and conditioned medium from treated macrophages was added. After 24 h of incubation, the migration of cells into the scratched area was assessed by analyzing images of 0- and 24-h time points by using ImageJ software. The percentage of cell migration was calculated by subtracting the 24-h value from the 0-h value, then dividing by the total area of the picture.

In vivo effects of AS1517499 in a 4T1 mammary carcinoma model

All animals (female, Balb/c, ~20 g) were purchased from Envigo (Indianapolis, IN, USA). Experimental protocols were approved by the Animal Ethical Committee of Utrecht University, The Netherlands. Animals were fed *ad libitum* and kept on a 12-h light/dark cycle. 4T1-luc cells (1×10^5) were injected into the mammary fat pad and tumors were allowed to develop. Tumor size was determined by using a Vernier caliper and tumor volume was calculated by using the formula: length × width^2 × 0.52. Treatment with AS1517499 (20 mg/kg i.p. twice per week) was started when the tumor volume reached a volume of ±100 mm^3. Before sacrificing, mice were injected with 3 mg D-luciferin (PerkinElmer) and imaged after 30 min using the in vivo imaging system.

Immunofluorescence

Formalin-fixed, paraffin-embedded human breast tumor tissue sections were anonymously provided by the Department of Pathology, LabPON (Enschede, The Netherlands). Ethical approvals were provided by the local medical ethical committee at LabPON. Use of human tissues for this study was approved by the local ethics committee (University of Twente). All experiments involving human tissues were performed in accordance with institutional guidelines and regulations. Four-micrometer sections were deparaffinized and antigens were retrieved by overnight incubation at 80°C in 0.1 M Tris-HCl (pH 9). Murine 5-μm cryosections were fixed in 4% formaldehyde. Sections were permeabilized in methanol at −20°C for 10 min. Sections were incubated with the primary Abs, pStat6, Stat6 (Cell Signaling Technology), and CD206 (Santa Cruz Biotechnology), overnight at 4°C. Secondary Abs that were labeled with Alexa Fluor 488 or Alexa Fluor

594 (Thermo Fisher Scientific) were incubated for 1 h. Stained sections were mounted by using mounting medium that contained DAPI anti-fade mounting medium (Sigma-Aldrich). Sections were subsequently scanned by using a NanoZoomer Digital slide scanner 2.0HT (Hamamatsu Photonics, Bridgewater, NJ, USA).

Statistical analysis

Data are presented as means + SEM. Graphs and statistical analyses were performed by using Prism (v.5.02; GraphPad Software, La Jolla, CA, USA). Data were analyzed by using an unpaired, 2-tailed Student's *t* test, unless otherwise specified. Differences were considered significant at a value of $P < 0.05$.

RESULTS

pStat6 expression in human and mouse breast tumors

To determine the expression of activated Stat6 [*i.e.*, phosphorylated Stat6 (pStat6)], we performed colocalization immunofluorescent staining in human breast tumor tissues and 4T1 mammary carcinoma tissue. Stat6 signaling was activated in both human and mouse breast tumor tissues in TAMs, as shown by the colocalization of pStat6 with $CD206^+$ macrophages (area marked M in **Fig. 1**). Tumors that were stained with pStat6 were positive for both estrogen and progesterone receptors. Of note, tumor cells did not express pStat6, as can be seen in the area marked T in Fig. 1.

Macrophage differentiation and pStat6 expression

To study whether the Stat6 pathway is specifically induced in M2, but not M1, we first differentiated the murine macrophage, RAW264.7, with IFN-γ and LPS for M1 and with IL-4 and IL-13 for M2 macrophages (TAM), then examined their different phenotypes. By using quantitative PCR, we confirmed the differentiation of M1 and M2 phenotypes with the induced M1 inflammatory markers (*Il-1β* and *Il-6*) and M2 markers [*Arg-1* (arginase-1) and *Mrc-1*; **Fig. 2*A***]. Furthermore, we examined the enzymatic activity in differentiated macrophages to confirm their distinct phenotypes (Fig. 2*B, C*). Arginase activity, measured by the quantification of urea as a side product of the conversion of L-arginine into L-ornithine, demonstrated higher activity in M2 macrophages compared with M1 macrophages (Fig. 2*B*). In contrast, NO_2^- production, as a result of induced NOS, was significantly increased only in M1 macrophages (Fig. 2*C*). As expected, we found that pStat6 was highly induced in M2 macrophages specifically (Fig. 2*D*). Although the undifferentiated or M1 macrophages had high expression levels of Stat6, no pStat6 expression was observed (Fig. 2*D*). In addition, 4T1 murine breast cancer cells also expressed Stat6, but not pStat6, which is in line with immunostaining data in human and mouse tumors (Fig. 1).

Stat6 gene silencing

To investigate whether Stat6 regulates M2 macrophage differentiation, we knocked down Stat6 by using an siRNA approach. We found that transfection of si-Stat6 reduced expression levels by 30% in M2 differentiated cells (**Fig. 3*A***). Of interest, the reduction of Stat6 expression significantly inhibited the differentiation of macrophages into the M2 type, as shown by the reduced expression of the *Mrc-1* gene, a marker for M2 type, and arginase-1 activity, a biochemical assay for M2-specific activity (Fig. 3). As arginase activity and *Mrc-1* gene expression are both elevated in M2 macrophages and have been established as reliable M2 markers, the decrease in these values after knocking down the *Stat6* gene confirmed the crucial

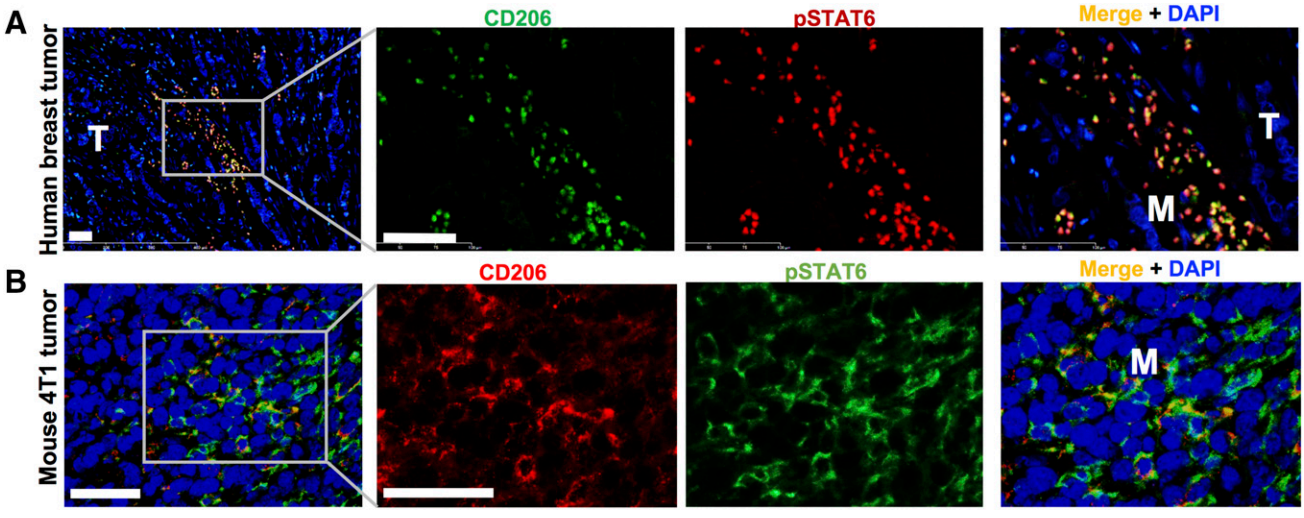

Figure 1. Representative fluorescent images showing coimmunostaining of pStat6 in human breast cancer and a murine 4T1 breast tumor model. *A*) pStat6 (red color) is colocalized mainly with $CD206^+$ macrophages (green). *B*) pStat6 (green) is colocalized with $CD206^+$ macrophages (red). T and M denote areas with tumor cells and a macrophage-rich area, respectively. Blue, DAPI. Scale bars, 50 μm.

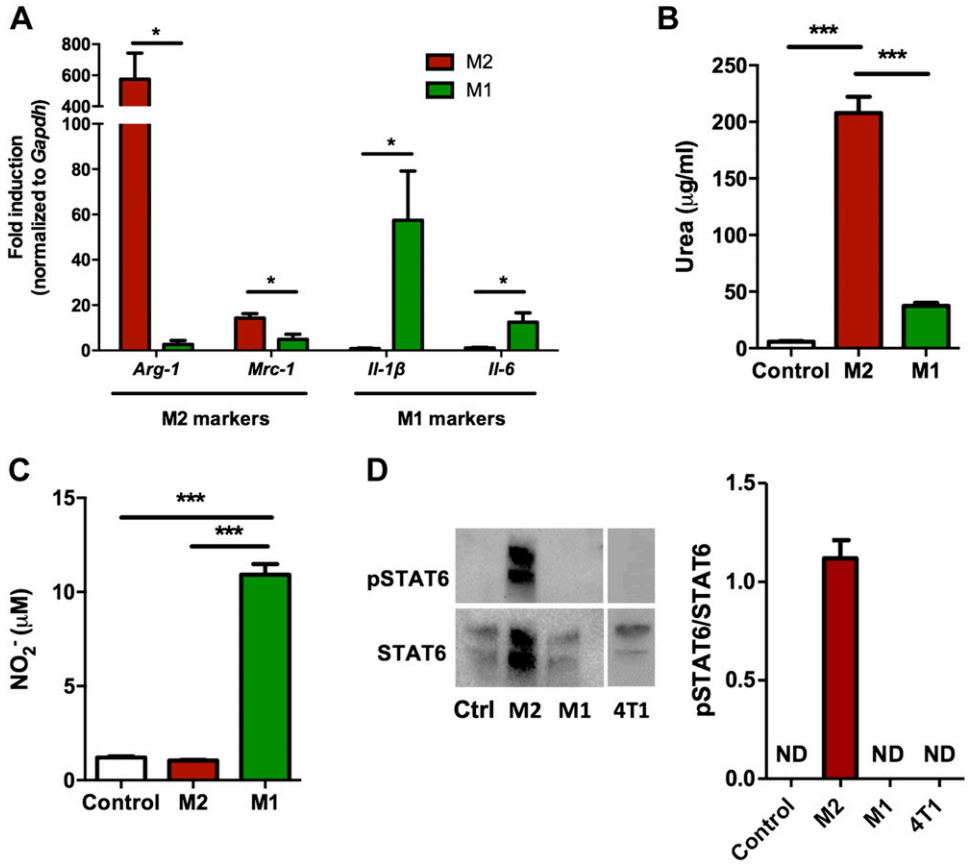

Figure 2. *In vitro* differentiation of murine macrophages into M2 and M1 macrophages. *A*) Quantitative real-time PCR analysis of macrophage differentiation. *B*) *Arg-1* activity in differentiated macrophages as measured by the amount of produced urea (μg/ml). *C*) Nitrite release assay in supernatants of differentiated macrophages (μM). *D*) Representative Western blot results and quantification showing that Stat6 phosphorylation is restricted to the M2 macrophage phenotype. Ctrl, undifferentiated control RAW264.7 cells. Bars represent means + SEM (n = 3–4). $^*P < 0.05$, $^{***}P < 0.001$.

role for this transcription factor in M2 macrophage differentiation.

Pharmacologic inhibition of Stat6 phosphorylation using AS1517499

After confirming that *Stat6* knockdown inhibits the differentiation of macrophages to the M2 type, we used a small drug molecule, AS1517499 (**Fig. 4*A***), to study whether the pharmacologic inhibition of Stat6 was also able to inhibit macrophage differentiation. As confirmed by Western blot analysis, treatment with AS1517499 inhibited the expression of pStat6 in M2 macrophages with increasing concentrations (Fig. 4*B*). In addition, AS1517499 inhibited M2 markers *Arg-1* and *Mrc-1* gene expression (Fig. 4*C*) and arginase activity in these cells with increasing concentrations (Fig. 4*D*). These data confirm that the pharmacologic inhibition of Stat6 using AS1517499 can inhibit M2 macrophage differentiation. In contrast, treatment of M1 macrophages with AS1517499 did not show any inhibition of M1 macrophages, but instead slightly activated them toward the M1 phenotype (Fig. 4*C*). As M1 macrophages are considered antitumoral macrophages, differentiation to the

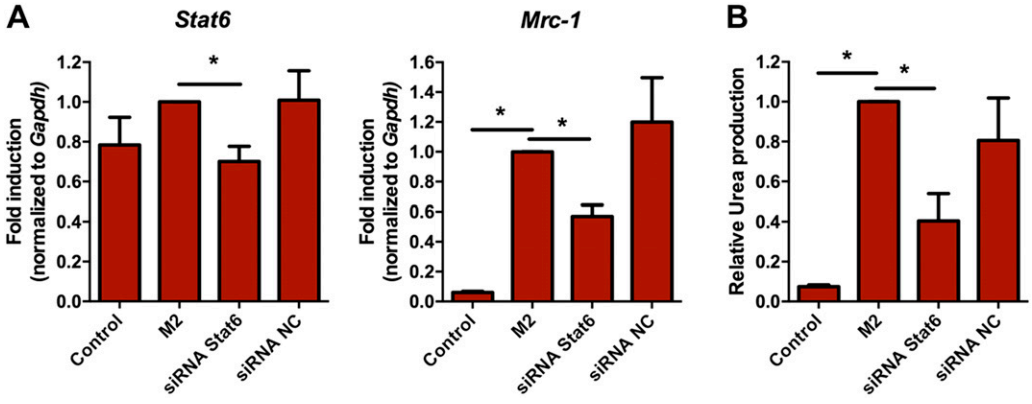

Figure 3. *In vitro* effects of *Stat6* gene silencing. *A*) Quantitative gene expression analysis depicting the inhibition of *Stat6* and *Mrc-1*. *B*) Inhibition of arginase activity by using *Stat6* siRNA. NC, noncoding. Bars represent means + SEM (n = 3). $^*P < 0.05$.

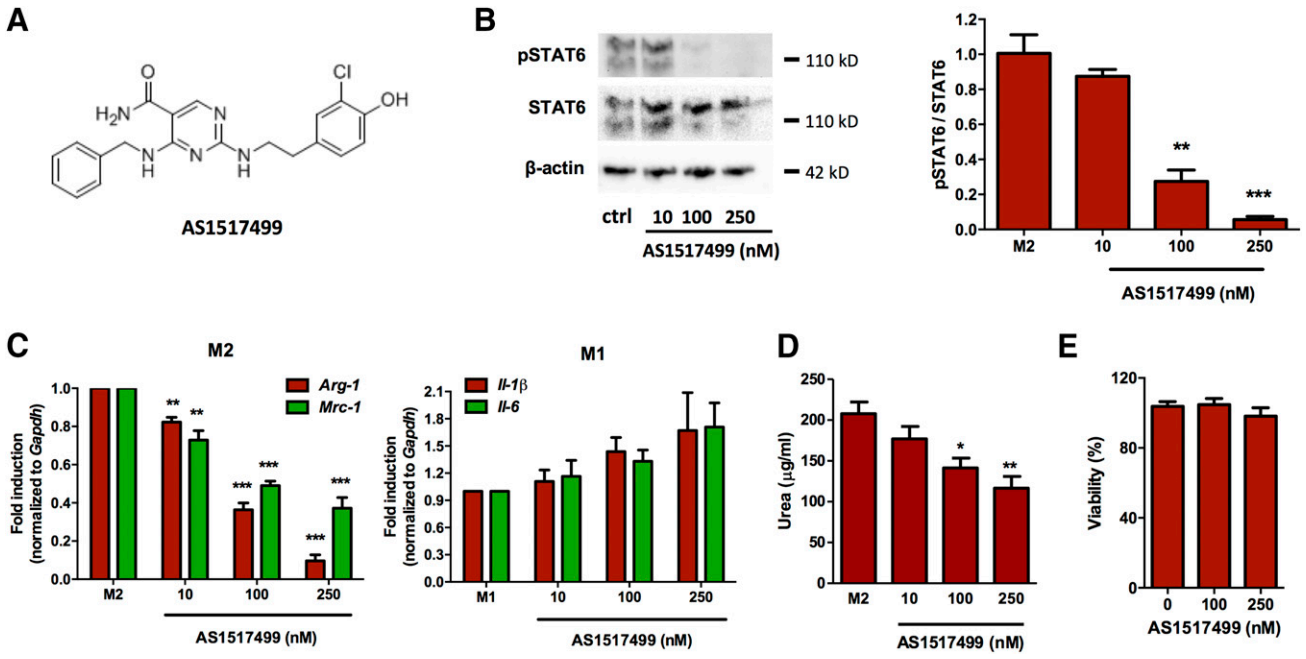

Figure 4. *In vitro* effects of the Stat6 inhibitor, AS1517499, in differentiated macrophages. *A*) Structure of the Stat6 inhibitor, AS1517499. *B*) Representative image and quantification of Western blot results of Stat6 phosphorylation in differentiated RAW264.7 cells that were treated with increasing concentrations of AS1517499. *C*) Real-time quantitative PCR results of macrophage differentiation with increasing concentrations of AS1517499 for M2 markers, *Arg-1* and *Mrc-1*, and M1 markers, *Il-1β* and *Il-6*. *D*) Inhibition of arginase activity using increasing concentrations of AS1517499. *E*) Cell viability of RAW264.7 cells that were incubated with AS1517499. Bars represent means + SEM ($n = 3$). $^*P < 0.05$, $^{**}P < 0.005$, $^{***}P < 0.001$.

M1 type can be of interest to achieve an antitumor effect. Of note, the concentrations of AS1517499 used also did not demonstrate any cytotoxicity in these cells (Fig. 4*E*).

AS1517499 inhibits tumor growth and metastasis in 4T1 mammary carcinoma model *in vivo*

To evaluate the effect of the Stat6 inhibitor, AS1517499, *in vivo*, we treated 4T1-luc tumor-bearing mice with the inhibitor (20 mg/kg, i.p., 2×/wk) when tumors became palpable. We found that treatment with AS1517499 significantly reduced tumor growth compared with vehicle-treated control mice (**Fig. 5*A***). At the end of the experiment, we quantified the tumor mass and potential liver metastasis by imaging the luciferase activity by using the IVIS *in vivo* imaging system. Of interest, mice that were treated with AS1517499 demonstrated a significant reduction in tumor mass compared with the vehicle-treated group, as can be seen in intact tumors in Fig. 5*B* and the quantification data in Fig. 5C. To rule out direct cytotoxic effects of AS1517499 on 4T1 cells, we examined cell viability at much higher concentrations, up to 4000 nM, compared with the effective concentration of 250 nM in macrophages and observed no decrease in cell viability (Fig. 5*D*). We examined the tumor gene expression of total and M2 macrophage markers [*F4/80* (EGF-like module-containing mucin-like hormone receptor-like 1), *Arg-1* and *Mrc-1*], but found no differences (data not shown); however, the intratumoral T-cell population marker displayed an increase in $CD8^+$ T cell gene expression and a slight increase in the CD4 regulatory T-cell marker, FoxP3 (forkhead box P3), whereas CD4 remained unchanged in the AS1517499-treated group compared with the vehicle-treated group (Fig. 5*E*).

We also studied the potential metastasis in the liver and found that the vehicle-treated group (4/6 positive) had more luminescence signal than the AS1517499-treated group (2/6 positive), as indicated by the scoring shown in the Fig. 5*F*. To determine whether M2 macrophages promote tumor cell migration and that the inhibition of Stat6 in these macrophages also inhibits a promigratory effect, we investigated the paracrine effects of M2 differentiated macrophages—with and without treatment with AS1517499—on tumor cell migration. We observed that the conditioned medium that was collected from M2 macrophages increased tumor cell migration compared with undifferentiated macrophages (Fig. 5*G*). Of importance, the conditioned medium collected from M2 macrophages that were treated with AS1517499 completely inhibited this M2 macrophage-induced tumor cell migration (Fig. 5*G*).

AS1517499 inhibits metastatic niche formation

As we observed an inhibitory effect of AS1517499 on early metastasis, we became interested in investigating whether AS1517499 could also inhibit metastatic niche formation in livers. We therefore set up a new experiment to track changes in the macrophage phenotype and metastatic niche markers with the progression of

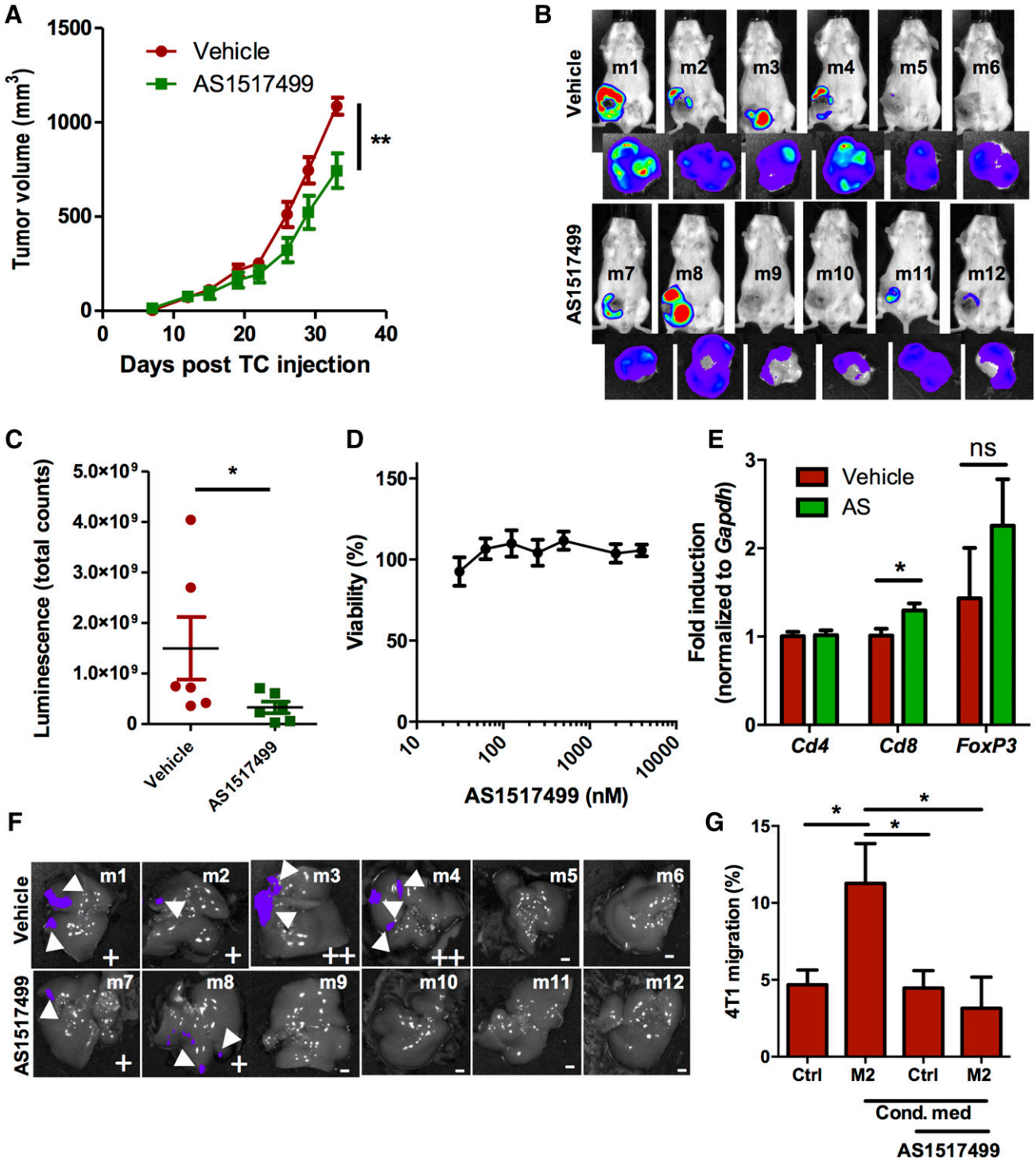

Figure 5. *In vivo* effect of AS1517499 treatment on tumor growth. *A*) Tumor volume of vehicle- and AS1517499-treated animals (20 mg/kg, i.p, 2×/wk) in days after tumor cell (TC) injection. *B*) IVIS *in vivo* imaging system images of untreated and treated mice before being euthanized and 15 min after luciferin injection. Isolated tumors are shown next to the respective mice. *C*) Quantitative data showing *ex vivo* tumor luminescence in the isolated tumors. *D*) Cell viability of 4T1 cells that were incubated with AS1517499. *E*) Quantitative real-time PCR results of T-cell markers (*Cd4*, *Cd8*, and *FoxP3*) in untreated and treated animals. *F*) Luminescence of livers after luciferin injection. Arrowheads indicate metastasis. Metastasis scoring (− no spots; + few spots of low intensity; ++ several spots) for livers is shown in the lower right corner of each image. *G*) Quantification of the migration of tumor cells 24 h after making the scratch. (*In vitro* experiments, $n = 3$–4; *in vivo* experiments, $n = 6$/group.) Data are shown as means + SEM. $^*P < 0.05$.

breast tumors. In this experiment, we collected livers from normal mice and 4T1 tumor-bearing mice with increasing tumor sizes (**Fig. 6*A***). We observed that the induction of tumors led to an increase of the general macrophage marker, *F4/80*, at an early stage, likely because of infiltrated macrophages (Fig. 6*B*). Increased tumor size led to an increase of M2 macrophage markers (*Mrc-1*, *Ym-1*), metastatic niche markers [*Mmp-2* (matrix

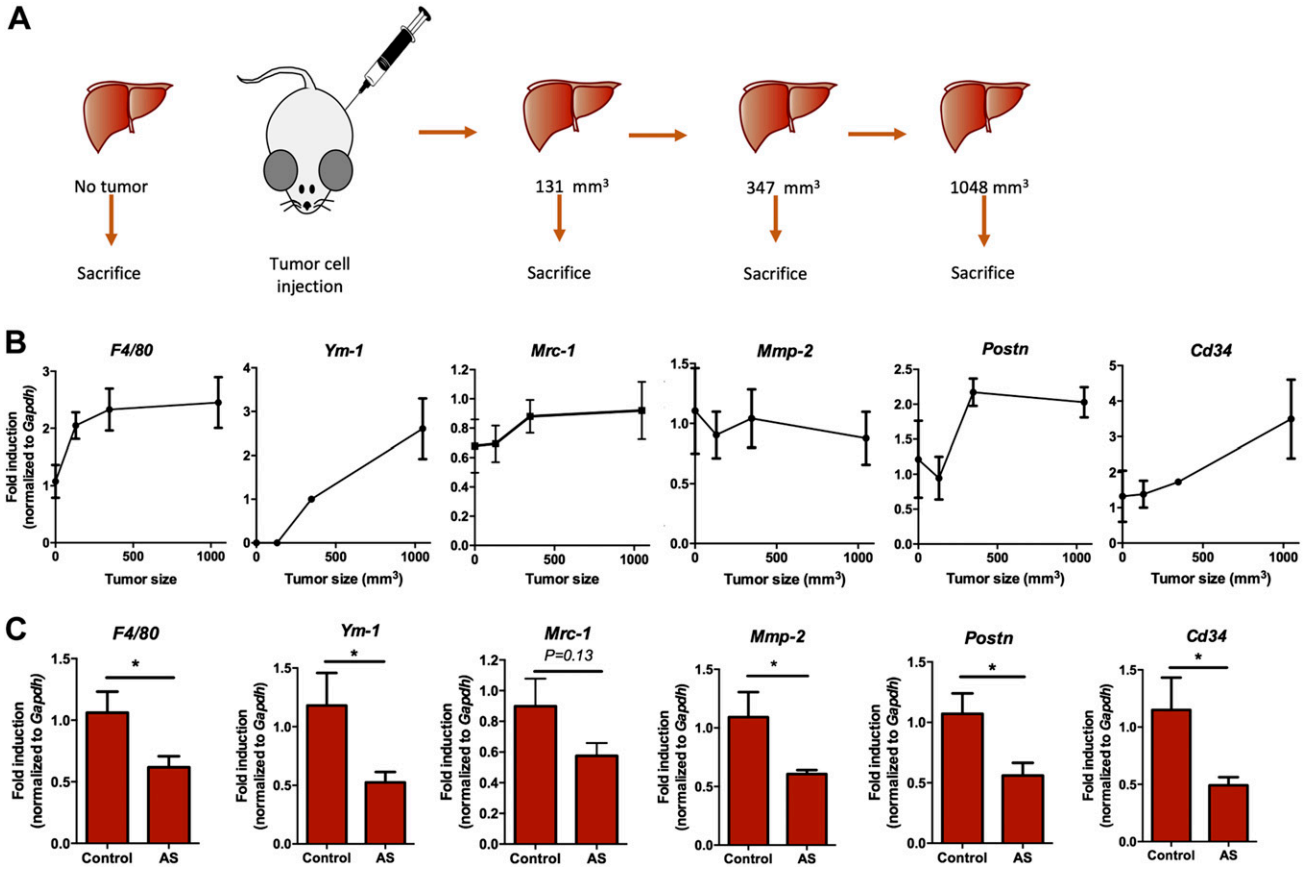

Figure 6. Macrophage and tumor progression markers measured in the livers of mice bearing tumors of increasing sizes and in animals treated or untreated with AS1517499. *A*) Experimental setup for tracking macrophage and metastatic markers in the livers of mice bearing increasing tumor sizes. Mice were euthanized before tumor development and when tumors reached the sizes of 131, 347, and 1048 mm^3 ($n = 3$/group). *B*) Gene expression analysis of macrophage (*F4/80*, *Ym-1*, and *Mrc-1*) and tumor progression markers (*Mmp-2*, *Postn*, and *Cd34*) in the livers of mice bearing tumors during tumor development. *C*) Macrophage and tumor progression markers in control- and AS1517499-treated animals ($n = 6$/group). Data are shown as means + SEM. $^*P < 0.05$.

metalloproteinase-2) and *Postn* (periostin)], and neoangiogenesis marker, *Cd34*, in liver (Fig. 6*B*). To assess whether Stat6 inhibition reduced the expression of metastatic niche markers in the liver, we examined these gene markers in the livers that were treated with AS1517499 from the experiment shown in Fig. 5. Of interest, we found that treatment with AS1517499 significantly inhibited the expression of metastatic niche markers (Fig. 6*C*). These data suggest that AS1517499 not only attenuates tumor growth, but also metastatic niche formation.

DISCUSSION

In this study, we demonstrate, for the first time to our knowledge, that the pharmacologic inhibition of Stat6 in TAMs by using a specific inhibitor (AS1517499) attenuates tumor growth and metastatic niche formation in breast cancer. Here, we confirm that Stat6 is expressed by TAMs in human breast tumors and is essential for the differentiation of the TAM phenotype (M2 type macrophages). The inhibition of Stat6 using an siRNA approach or AS1517499 inhibited M2 differentiation *in vitro*. Furthermore, treatment with AS1517499 not only attenuated tumor growth, but early metastasis in a syngeneic 4T1 mammary carcinoma mouse model. Subsequently, we demonstrated that several gene markers that are related to the macrophage and metastatic niche were induced in the liver, with increasing growth of the primary tumor in mice. Of interest, treatment with AS1517499 significantly inhibited these metastatic niche markers in the liver. This study underlines the importance of the Stat6 pathway in TAM differentiation and suggests that the inhibition of this pathway may be an interesting way by which to block TAM-induced protumorigenic effects.

TAMs display a number of protumoral functions, including extracellular matrix remodeling, neoangiogenesis, suppression of adaptive immunity, and facilitate tumor metastasis (12). Differentiation of infiltrated macrophages into the TAM phenotype *via* IL-4/IL-13 cytokines is well known and, therefore, their intrinsic pathway—that is, the Stat6 pathway is a key target to intervene in TAM-induced tumor processes. In the present study, we show that pStat6 (activated form) was abundantly present in TAMs in both human breast tumor tissue and 4T1 tumors in mice, as shown by immunofluorescent staining (Fig. 1). In addition, *in vitro*, the Stat6 pathway was specifically activated in M2 differentiated cells compared with M1 cells. Jia *et al.* (27) have previously demonstrated that the activation of macrophages with 4T1 conditioned medium leads to the

induction of the pStat6 pathway . Our data that demonstrate the inhibition of the differentiation of macrophages to M2 type after Stat6 silencing using siRNA confirm that the Stat6 pathway is a key regulatory pathway in this process. To apply the Stat6 inhibition strategy pharmacologically *in vivo*, we used the Stat6 inhibitor, AS1517499, which was previously reported to be a potent Stat6-specific inhibitor in nonmalignant diseases (24–26). In our study, AS1517499 displayed a strong inhibition of Stat6 phosphorylation at nanomolar concentrations and inhibited M2 differentiation, as shown with the inhibition of M2-related markers (*Arg-1* and *Mrc-1*) and enzyme activity.

In vivo, after treatment with AS1517499, tumor growth slowed down in 5 of 6 mice compared with the vehicle-treated group. In the vehicle-treated group, all mice had a consistently high growth rate (Fig. 5*A*). As these tumors often become hypoxic and necrotic, we included the 4T1-luciferase–induced luminescence signal to represent the effect on tumor mass and observed a high reduction in tumor mass. Although *in vitro* we showed that AS1517499 inhibited M2 differentiation, the *in vivo* effect might be a result of cytotoxicity to tumor cells directly. The latter was ruled out when, at a much higher concentration, AS1517499 demonstrated no cytotoxicity to 4T1 cells (Fig. 5*D*). Moreover, pStat6 expression was also absent in 4T1 cells (Fig. 2*D*), which indicated that the reduction in tumor growth after treatment with AS1517499 was not a result of the direct effect of the inhibitor on tumor cells. To examine whether M2 macrophages induce tumor cell growth in a paracrine manner, we examined the effect of the conditioned medium that was collected from M2 macrophages on 4T1 cell growth and found no induction of cell growth (data not shown). In tumors, we also observed no change in the gene expression of M2 markers after treatment with AS1517499. Ostrand-Rosenberg *et al.* (22) previously demonstrated that when *Stat6*$^{-/-}$ mice were challenged with 4T1 tumor cells, the mice demonstrated a delay in primary tumor growth and a reduction in metastasis. These effects were found to be independent of $CD4^+$ cells, but were a result of elevated levels of $CD8^+$ cells in tumors. In agreement with the latter study, we also found that tumors that were treated with AS1517499 had an induced expression of CD8, but not CD4, which indicates that treatment with AS1517499 might have reduced tumor growth by inhibiting TAM-induced immune suppression.

A crucial finding of the present study is the reduction of liver metastasis resulting from treatment with AS1517499, as most cancer-related mortalities occur as a result of metastasis. TAMs are known to induce tumor cell migration (28–30), which was also confirmed in this study. Furthermore, we showed that inhibition of TAM (M2 macrophages) with AS1517499 inhibited tumor migration. To this end, we wondered whether AS1517499 only inhibited tumor cell migration or also metastatic niche formation at the metastatic site (*i.e.*, liver). Several studies that were summarized in a recent review by Peinado *et al.* (31) demonstrated that tumor cells secrete extracellular vesicles and growth factors at the primary tumor site, which migrate to metastatic sites and establish a premetastatic niche to harbor and nourish tumor cells. To examine the effect of AS1517499 on the metastatic niche in the liver, we first examined which genes are induced and/or altered in the liver during 4T1 tumor development. Our data show an increase in the gene expression of total (*F4/80*) and M2 macrophages (*Ym-1* and *Mrc-1*) and other metastatic markers (*Mmp-2*, *Postn*, and *Cd34*) in the liver (Fig. 6*B*). Recruitment of infiltrated macrophages and activation of resident Kupffer cells are known to be crucial processes in premetastatic niche formation (31). MMP2 plays an important role in organizing the extracellular matrix of the metastatic niche (32). Periostin is an extracellular matrix protein that has been shown to be associated with the premetastatic niche. Malanchi *et al.* (33) demonstrated that periostin serves to concentrate and present Wnt ligands, thereby inducing and maintaining stem-like metastasis founder cells. Recently, periostin was shown to be secreted by glioblastoma stem cells, which resulted in increased recruitment and differentiation of TAMs (34). During metastasis, bone marrow–derived cells have been shown to infiltrate and express CD34 (35) and, in addition to that, endothelial cells also express CD34, which is known to participate in establishing the metastatic niche. Of interest, AS1517499-treated mice displayed reduced expression of macrophage markers, which suggests a reduction in intrahepatic macrophage infiltration and an increased M2-driven macrophage polarization. Furthermore, AS1517499 also inhibited the expression of *Mmp-2*, *Postn*, and *Cd34*, key genes in metastasis formation. Nevertheless, it remains to be investigated whether the reduction of these key mediators with AS1517499 is a direct effect or a consequence of the inhibition of the primary tumor.

In summary, we demonstrate that the inhibition of the Stat6 pathway in TAMs using AS1517499 leads to reduced tumor growth and metastasis. As M2 macrophages induce protumorigenic effects both at the primary tumor site and the metastatic site, the inhibition of the Stat6 pathway in these macrophages can provide dual effects to abrogate both tumor growth and metastasis development, as shown in this study. Furthermore, the combination of AS1517499 with other anticancer agents (*e.g.*, chemotherapy and immunotherapy) might be of interest to potentiate their therapeutic efficacy. Taken together, the inhibition of Stat6 using AS1517499 is a promising approach to dampen the protumorigenic effects of TAMs and should be explored as a potential adjuvant therapy for the treatment of breast cancer. FJ

ACKNOWLEDGMENTS

The authors thank Dr. Joop van Baarlen (LabPON, Hengelo, The Netherlands) for providing human breast tumor tissue. This study was supported by the Phospholipid Research Centre Heidelberg (Grant 30926319 to J.P.) and the MIRA Institute, University of Twente. The authors declare no conflicts of interest.

AUTHOR CONTRIBUTIONS

K. Binnemars-Postma and R. Bansal performed the experiments; K. Binnemars-Postma and J. Prakash designed the study, analyzed the data, and wrote the

paper; and G. Strom reviewed the paper and provided comments.

REFERENCES

1. International Agency for Research on Cancer. Breast cancer, estimated incidence, mortality and prevalence worldwide in 2012. Accessed June 24, 2017, at http://globocan.iarc.fr/old/FactSheets/cancers/breast-new.asp
2. Tang, X. (2013) Tumor-associated macrophages as potential diagnostic and prognostic biomarkers in breast cancer. *Cancer Lett.* **332**, 3–10
3. Oishi, K., Sakaguchi, T., Baba, S., Suzuki, S., and Konno, H. (2014) Macrophage density and macrophage colony-stimulating factor expression predict the postoperative prognosis in patients with intrahepatic cholangiocarcinoma. *Surg. Today* **45**, 715–722
4. Ding, T., Xu, J., Wang, F., Shi, M., Zhang, Y., Li, S. P., and Zheng, L. (2009) High tumor-infiltrating macrophage density predicts poor prognosis in patients with primary hepatocellular carcinoma after resection. *Hum. Pathol.* **40**, 381–389
5. Mantovani, A., Allavena, P., and Sica, A. (2004) Tumour-associated macrophages as a prototypic type II polarised phagocyte population: role in tumour progression. *Eur. J. Cancer* **40**, 1660–1667
6. Wang, N., Liang, H., and Zen, K. (2014) Molecular mechanisms that influence the macrophage M1-M2 polarization balance. *Front. Immunol.* **5**, 614
7. Sica, A., Schioppa, T., Mantovani, A., and Allavena, P. (2006) Tumour-associated macrophages are a distinct M2 polarised population promoting tumour progression: potential targets of anti-cancer therapy. *Eur. J. Cancer* **42**, 717–727
8. Noy, R., and Pollard, J. W. (2014) Tumor-associated macrophages: from mechanisms to therapy. *Immunity* **41**, 49–61
9. Sica, A., and Mantovani, A. (2012) Macrophage plasticity and polarization: *in vivo* veritas. *J. Clin. Invest.* **122**, 787–795
10. Sica, A., Allavena, P., and Mantovani, A. (2008) Cancer related inflammation: the macrophage connection. *Cancer Lett.* **267**, 204–215
11. Mantovani, A., Marchesi, F., Malesci, A., Laghi, L., and Allavena, P. (2017) Tumour-associated macrophages as treatment targets in oncology. *Nat. Rev. Clin. Oncol.* **14**, 399–416
12. Allavena, P., and Mantovani, A. (2012) Immunology in the clinic review series; focus on cancer: tumour-associated macrophages: undisputed stars of the inflammatory tumour microenvironment. *Clin. Exp. Immunol.* **167**, 195–205
13. Biswas, S. K., Allavena, P., and Mantovani, A. (2013) Tumor-associated macrophages: functional diversity, clinical significance, and open questions. *Semin. Immunopathol.* **35**, 585–600
14. Brown, H. K., and Holen, I. (2009) Anti-tumour effects of bisphosphonates—what have we learned from *in vivo* models? *Curr. Cancer Drug Targets* **9**, 807–823
15. Zeisberger, S. M., Odermatt, B., Marty, C., Zehnder-Fjällman, A. H., Ballmer-Hofer, K., and Schwendener, R. A. (2006) Clodronate-liposome-mediated depletion of tumour-associated macrophages: a new and highly effective antiangiogenic therapy approach. *Br. J. Cancer* **95**, 272–281
16. Ngambenjawong, C., Gustafson, H. H., and Pun, S. H. (2017) Progress in tumor-associated macrophage (TAM)-targeted therapeutics. *Adv. Drug Deliv. Rev.* **114**, 206–221
17. Hume, D. A., and MacDonald, K. P. (2012) Therapeutic applications of macrophage colony-stimulating factor-1 (CSF-1) and antagonists of CSF-1 receptor (CSF-1R) signaling. *Blood* **119**, 1810–1820
18. Pyonteck, S. M., Akkari, L., Schuhmacher, A. J., Bowman, R. L., Sevenich, L., Quail, D. F., Olson, O. C., Quick, M. L., Huse, J. T., Teijeiro, V., Setty, M., Leslie, C. S., Oei, Y., Pedraza, A., Zhang, J., Brennan, C. W., Sutton, J. C., Holland, E. C., Daniel, D., and Joyce, J. A. (2013) CSF-1R inhibition alters macrophage polarization and blocks glioma progression. *Nat. Med.* **19**, 1264–1272
19. Quail, D. F., Bowman, R. L., Akkari, L., Quick, M. L., Schuhmacher, A. J., Huse, J. T., Holland, E. C., Sutton, J. C., and Joyce, J. A. (2016) The tumor microenvironment underlies acquired resistance to CSF-1R inhibition in gliomas. *Science* **352**, aad3018
20. Nelms, K., Keegan, A. D., Zamorano, J., Ryan, J. J., and Paul, W. E. (1999) The IL-4 receptor: signaling mechanisms and biologic functions. *Annu. Rev. Immunol.* **17**, 701–738
21. Pauleau, A. L., Rutschman, R., Lang, R., Pernis, A., Watowich, S. S., and Murray, P. J. (2004) Enhancer-mediated control of macrophage-specific arginase I expression. *J. Immunol.* **172**, 7565–7573
22. Ostrand-Rosenberg, S., Grusby, M. J., and Clements, V. K. (2000) Cutting edge: STAT6-deficient mice have enhanced tumor immunity to primary and metastatic mammary carcinoma. *J. Immunol.* **165**, 6015–6019
23. Liao, X., Sharma, N., Kapadia, F., Zhou, G., Lu, Y., Hong, H., Paruchuri, K., Mahabeleshwar, G. H., Dalmas, E., Venteclef, N., Flask, C. A., Kim, J., Doreian, B. W., Lu, K. Q., Kaestner, K. H., Hamik, A., Clément, K., and Jain, M. K. (2011) Krüppel-like factor 4 regulates macrophage polarization. *J. Clin. Invest.* **121**, 2736–2749
24. Nagashima, S., Yokota, M., Nakai, E., Kuromitsu, S., Ohga, K., Takeuchi, M., Tsukamoto, S., and Ohta, M. (2007) Synthesis and evaluation of 2-[2-(4-hydroxyphenyl)-ethyl]aminopyrimidine-5-carboxamide derivatives as novel STAT6 inhibitors. *Bioorg. Med. Chem.* **15**, 1044–1055
25. Sakurai, M., Nishio, M., Yamamoto, K., Okuda, T., Kawano, K., and Ohnuki, T. (2003) TMC-264, a novel inhibitor of STAT6 activation produced by Phoma sp. TC 1674. *J. Antibiot.* **56**, 513–519
26. Chiba, Y., Todoroki, M., Nishida, Y., Tanabe, M., and Misawa, M. (2009) A novel STAT6 inhibitor AS1517499 ameliorates antigen-induced bronchial hypercontractility in mice. *Am. J. Respir. Cell Mol. Biol.* **41**, 516–524
27. Jia, X., Yu, F., Wang, J., Iwanowycz, S., Saaoud, F., Wang, Y., Hu, J., Wang, Q., and Fan, D. (2014) Emodin suppresses pulmonary metastasis of breast cancer accompanied with decreased macrophage recruitment and M2 polarization in the lungs. *Breast Cancer Res. Treat.* **148**, 291–302
28. Condeelis, J., and Pollard, J. W. (2006) Macrophages: obligate partners for tumor cell migration, invasion, and metastasis. *Cell* **124**, 263–266
29. Solinas, G., Schiarea, S., Liguori, M., Fabbri, M., Pesce, S., Zammataro, L., Pasqualini, F., Nebuloni, M., Chiabrando, C., Mantovani, A., and Allavena, P. (2010) Tumor-conditioned macrophages secrete migration-stimulating factor: a new marker for M2-polarization, influencing tumor cell motility. *J. Immunol.* **185**, 642–652
30. Guo, Q., Jin, Z., Yuan, Y., Liu, R., Xu, T., Wei, H., Xu, X., He, S., Chen, S., Shi, Z., Hou, W., and Hua, B. (2016) New mechanisms of tumor-associated macrophages on promoting tumor progression: recent research advances and potential targets for tumor immunotherapy. *J. Immunol. Res.* **2016**, 9720912
31. Peinado, H., Zhang, H., Matei, I. R., Costa-Silva, B., Hoshino, A., Rodrigues, G., Psaila, B., Kaplan, R. N., Bromberg, J. F., Kang, Y., Bissell, M. J., Cox, T. R., Giaccia, A. J., Erler, J. T., Hiratsuka, S., Ghajar, C. M., and Lyden, D. (2017) Pre-metastatic niches: organ-specific homes for metastases. *Nat. Rev. Cancer* **17**, 302–317
32. Erler, J. T., Bennewith, K. L., Cox, T. R., Lang, G., Bird, D., Koong, A., Le, Q. T., and Giaccia, A. J. (2009) Hypoxia-induced lysyl oxidase is a critical mediator of bone marrow cell recruitment to form the pre-metastatic niche. *Cancer Cell* **15**, 35–44
33. Malanchi, I., Santamaria-Martínez, A., Susanto, E., Peng, H., Lehr, H. A., Delaloye, J. F., and Huelsken, J. (2011) Interactions between cancer stem cells and their niche govern metastatic colonization. *Nature* **481**, 85–89
34. Zhou, W., Ke, S. Q., Huang, Z., Flavahan, W., Fang, X., Paul, J., Wu, L., Sloan, A. E., McLendon, R. E., Li, X., Rich, J. N., and Bao, S. (2015) Periostin secreted by glioblastoma stem cells recruits M2 tumour-associated macrophages and promotes malignant growth. *Nat. Cell Biol.* **17**, 170–182
35. Kaplan, R. N., Riba, R. D., Zacharoulis, S., Bramley, A. H., Vincent, L., Costa, C., MacDonald, D. D., Jin, D. K., Shido, K., Kerns, S. A., Zhu, Z., Hicklin, D., Wu, Y., Port, J. L., Altorki, N., Port, E. R., Ruggero, D., Shmelkov, S. V., Jensen, K. K., Rafii, S., and Lyden, D. (2005) VEGFR1-positive haematopoietic bone marrow progenitors initiate the pre-metastatic niche. *Nature* **438**, 820–827

Received for publication July 5, 2017.
Accepted for publication October 10, 2017.